



Accurate determination of X-ray energies using powder diffraction

N.A. Rae, C.T. Chantler*, C.Q. Tran, Z. Barnea

School of Physics, University of Melbourne, Victoria 3010, Australia

Accepted 21 September 2005

Abstract

We report synchrotron energy determinations using the powder diffraction patterns of Si (640b) and LaB₆ (660) standard reference powders at a number of energies between 5 and 20 keV. The fitted peak positions of all peaks recorded on image plates were used in each energy determination. Several sources of systematic error were investigated and their connection led to physically reasonable and consistent fitting parameters. The energies were determined to better than 0.025% at all energies. Our procedure shows that the use of the accurately known lattice parameters of standard materials makes it possible to determine X-ray energies without involving the full panoply of the Rietveld technique (which involves the crystal structure, crystal perfection, particle size, preferred orientation and other parameters affecting the full powder diffraction pattern).

© 2006 Elsevier Ltd. All rights reserved.

PACS: 61.12.Nz; 07.85.Qe; 41.50.+h

Keywords: Powder diffraction; Synchrotron radiation

1. Introduction

Synchrotron radiation sources provide a continuum of X-ray energies. The ability to monochromate the beam to a particular energy with a very narrow energy width has greatly broadened the field of X-ray spectroscopy. Powder diffraction is a widely used technique at synchrotrons and is often used to determine energy. While single crystals often have narrower diffraction peaks and a more accurate final determination of the X-ray energy under ideal conditions, powder diffraction techniques can quickly measure the full powder pattern. Determining energy from the entire powder pattern,

rather than from selected peaks, provides information about key systematic errors. By using all of the peaks and using the entire energy range, the different errors can be readily separated.

Powder patterns of the Si (SRM640b) and LaB₆ (SRM660) standard powders (unsorted as to particle size) were recorded using image plates at 23 energies between 5 and 20 keV. The 640 and 660 series are the most accurate powder standards available: $a_0 = 5.430940(11)\text{\AA}$ for silicon 640b (Parrish et al., 1999) and $a_0 = 4.15695(6)\text{\AA}$ for lanthanum hexaboride 660 (Rasberry et al., 1989). The diffraction pattern was recorded in 8 mm wide strips on six X-ray image plates mounted in Big Diff, a large cylindrical diffraction chamber with the Debye–Scherrer geometry (Barnea et al., 1992). The glass capillary tubes filled with the powders were spun to average over crystal orientations. Radioactive fiducials on the perimeter of the

*Corresponding author. Fax: +61 3 83445437.

E-mail address: chantler@ph.unimelb.edu.au
(C.T. Chantler).

diffraction chamber gave a calibrated signature for the plate locations.

The energies were used as part of the X-ray extended range technique to measure the mass attenuation coefficient of pure elemental samples of silver, copper and gold (Chantler et al., 2001, 2003).

2. Analysis of the diffraction pattern

Diffraction peaks were fitted with a nonlinear least squares fit of a lorentzian convolved with a slit on a quadratic background. Peak centroids were determined to a precision between 0.001° and 0.0001° . Reduced χ_r^2 values varied from 1 to 10 for a typical energy, owing to background noise and structure, and occasionally due to the effect of nearby peaks.

Analysis has been automated, so that all peaks were indexed and fitted for energy. In past studies (Chantler et al., 2004), peaks have often been discarded particularly at the highest and lowest angles in the course of the energy determination. Sometimes this was due to background structure; increasing noise for high-index peaks; or due to the anomalous widths or centroids of low index peaks. Our approach manages to retain all the diffraction peaks in a coherent and consistent peak fitting procedure.

The full powder pattern was indexed using the peak centroid positions. For high angle peaks, the difference between successive permitted Bragg indices became comparable with the systematic errors affecting the peak position. To correct for this, the largest source of error, the image plate offset was varied while the energy was calculated for each peak using the Bragg equation. The standard deviation of the fitted energies was then minimized by varying peak indices. This method proved to be a robust way of indexing the pattern with the result that none of the peaks had to be discarded.

The peak angular positions are offset due to the six image plate offsets $\delta\theta_{pi}$ and the eccentricity of the powder sample. Eccentricity of the powder sample from the centre of the diffraction chamber is due to a vertical offset $\delta\theta_y$ and a horizontal offset $\delta\theta_z$. For small angles these are

$$\delta\theta_y = \frac{\delta_y}{D} \cos 2\theta, \quad \delta\theta_z = \frac{\delta_z}{D} \sin 2\theta, \quad (1)$$

where D is the diameter of the diffraction chamber. These forms of δ_y and δ_z orthogonalize the components and minimize correlations between the two parameters. To determine the energy of the beam, we fitted the angular offset of peaks with the nominal energy E of the incident beam,

$$\arcsin\left(\frac{hc}{2d(E + \delta E)}\right) = \theta + \delta\theta_{pi} + \frac{\delta_y}{D} \cos 2\theta + \frac{\delta_z}{D} \sin 2\theta. \quad (2)$$

There are nine free parameters in this procedure. Image plate displacements affect only peaks occurring on a given plate, while δE (the correction to the nominal energy), $\delta\theta_y$ and $\delta\theta_z$ affect all peaks. This makes it important to fit all of the peaks simultaneously because the correlation between $\delta\theta_y$ and $\delta\theta_{pi}$ for each image plate is different. In order to reduce the correlation between the parameters we measured multiple image plates. Other possible image plate offsets, due to the stretching of the plate during digitization and due to digitization at an angle to the plane of the strip in which the diffraction pattern was recorded, were investigated and found to be negligible in all cases.

The fitting procedure used an implementation of the Levenberg–Marquardt technique to fit θ_{meas} to the nonlinear Eq. (2). A typical plot of the residuals for one energy is shown in Fig. 1 for lanthanum hexaboride and in Fig. 2 for silicon.

Wherever χ_r^2 values of the energies were greater than one, one-sigma error bars were scaled with χ_r^2 values. The largest correction was due to inaccuracies in the positions of the radioactive fiducials (markers) of the six image plates $\delta\theta_{pi}$. This contributed shifts of up to 0.04° per plate.

The fitting procedure was repeated with δ_z included. As δ_z is in the direction of the incident beam, it is expected that this parameter is correlated with the fitted energy because of linear attenuation. χ_r^2 was significantly reduced when $\delta\theta_z$ was included in the fits, for example from 2.4 to 2.2 for the lanthanum hexaboride data in Fig. 1, and from 7.5 to 6.3 for the silicon data in Fig. 2. At low energies, the uncertainty in δ_z is greater due to the smaller number of available peaks. The value of δ_z was consistently $40\text{--}50\ \mu\text{m}$ and therefore a physically meaningful parameter.

Each experimental energy was fitted independently, and then used to fit a calibration curve for the

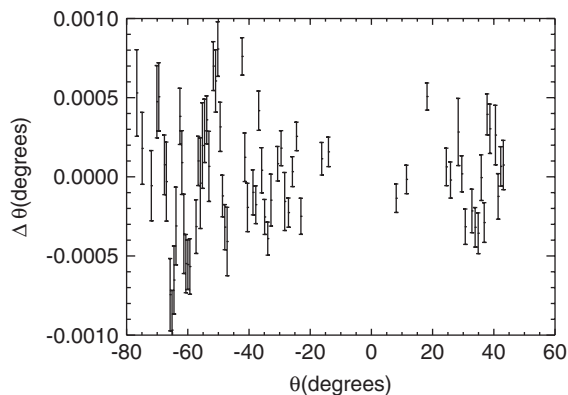


Fig. 1. An example of lanthanum hexaboride peak angle residuals after fitting: $E = 20\ \text{keV}$, 69 peaks. Note the narrow range of residuals and the consistency within a few σ for each peak.

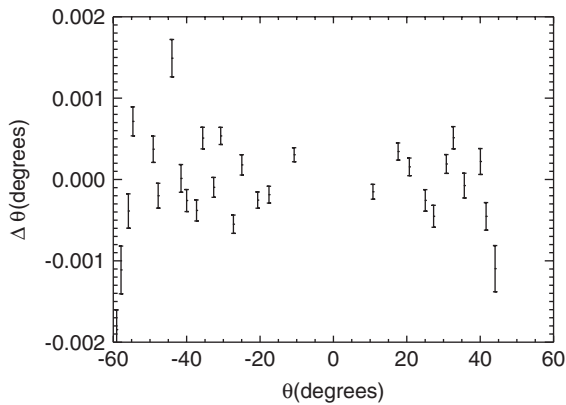


Fig. 2. Typical silicon peak angle residuals after fitting: $E = 20$ keV, 27 peaks. Silicon has fewer peaks than LaB_6 but the lattice spacing is known to better accuracy.

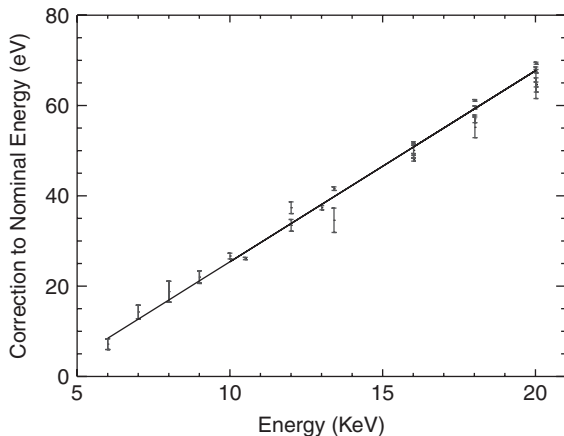


Fig. 3. Corrections to the nominally calibrated beam energy from the powder diffraction energy determination versus the nominal beam energy.

monochromator angle. Fig. 3 shows the calibration curve interpolated over the energy range. The data were well fitted with a linear equation, perhaps a surprising result given the nonlinear response curves often reported. The fitted curve agrees with the data within errors, which suggests that the random hysteresis of the monochromator was correctly minimized by approaching the desired angle consistently from the same direction. The fitted energies for both powders are listed in Table 1.

3. Conclusion

By matching the powder diffraction spectrum using fitted peak centroids, the energy of the synchrotron X-ray beam was successfully determined to high precision.

Table 1

Energy determinations (eV) from this investigation (the first series is for the Cu experiment, then for Au, and the last is for the Ag experiment) fitted without a horizontal eccentricity offset but with the optimized fitting procedure

| E_{nom} | $E_{\text{cal,Si}}$ | $\sigma_{E_{\text{cal,Si}}}$ | $E_{\text{cal,LaB}_6}$ | $\sigma_{E_{\text{cal,LaB}_6}}$ |
|------------------|---------------------|------------------------------|------------------------|---------------------------------|
| 20021.3 | 20085.97 | 0.53 | 20090.67 | 0.22 |
| 18017.0 | 18074.01 | 0.85 | 18078.08 | 0.19 |
| 16011.4 | 16060.28 | 0.49 | 16063.15 | 0.20 |
| 20023.0 | 20087.60 | 1.57 | 20090.55 | 0.40 |
| 18018.5 | 18074.77 | 2.29 | 18079.11 | 0.32 |
| 16012.7 | 16060.84 | 1.11 | 16062.81 | 0.38 |
| 20015.6 | 20073.72 | 0.56 | 20080.81 | 0.42 |
| 13407.5 | 13446.06 | 0.38 | 13446.37 | 0.09 |
| 12005.8 | 12038.85 | 0.32 | 12040.27 | 0.28 |
| 10505.0 | 10531.49 | 0.40 | 10532.78 | 0.33 |
| 9003.9 | – | – | 9024.20 | 0.17 |
| 8003.5 | – | – | 8021.59 | 0.56 |
| 7002.6 | – | – | 7016.75 | 0.16 |
| 6002.3 | – | – | 6014.02 | 0.21 |

Measurements in the central range are robust and consistent with low uncertainty. At low energies there were insufficient peaks per plate for a full investigation using the silicon powder.

The accuracy of the determination was increased by fitting all of the diffraction peaks consistently, in a robust and automated procedure. Systematic errors were investigated using the powder patterns obtained at the various energies. Fitted parameters were found to have consistent, physically meaningful values in all the energy determinations.

This method is a development of Chantler et al., 2004. Unlike the Rietveld, 1969 method which requires knowledge of the structure, thermal parameters, perfection and particle size, preferred orientation and other parameters affecting the full powder diffraction pattern, our traditional technique requires principally accurate lattice parameters of the standard powders. This technique is rapid, accurate and largely automatic.

Large differences for the determined energy have been found in such careful analysis compared to a dependence on the standard monochromator calibrations as demonstrated in Fig. 3.

Careful calibration of the delivered synchrotron beam in the hutch should always be performed for experiments requiring significant accuracy.

Acknowledgements

The authors acknowledge the experimental team and the local ANBF staff, particularly James Hester, as well as funding from the ASRP and ARC.

References

- Barnea, Z., Creigh, D.C., Davis, T.J., Garrett, R.F., Janky, S., Stevenson, A.W., Wilkins, S.W., 1992. The Australian diffractometer at the photon factory. *Rev. Sci. Instrum.* 63, 1069, 5.
- Chantler, C.T., Tran, C.Q., Barnea, Z., Paterson, D., Cookson, D.J., Balaic, D.X., 2001. X-ray extended-range technique for precision measurement of the X-ray mass attenuation coefficient and $\text{Im}(f)$ for copper using synchrotron radiation. *Phys. Rev. A* 64, 062506.
- Chantler, C.T., Tran, C.Q., Barnea, Z., Paterson, D., Cookson, D.J., 2003. Measurement of the X-ray mass attenuation coefficient and the imaginary part of the form factor of silicon using synchrotron radiation. *Phys. Rev. A* 67, 042716.
- Chantler, C.T., Tran, C.Q., Cookson, D.J., 2004. Precise measurement of the lattice spacing of LaB_6 standard powder by the X-ray extended range technique using synchrotron radiation. *Phys. Rev. A* 69, 042101.
- Parrish, W., Wilson, A.J.C., Langford, J.I., in: Wilson, A.J.C., Prince, E. (Eds.), *International Table for X-ray Crystallography*, vol. C, Kluwer Academic, 1999, Section 5.2.10.
- Rasberry, S.D., Hubbard, C.R., Zhang, Y., McKenzie, R.L., noted therein, 1989. National Institute of Standards and Technology SRM Certificates, Standard Reference Materials 660.
- Rietveld, H.M., 1969. A profile refinement method for nuclear and magnetic structures. *J. Appl. Cryst.* 2, 65.